
Graphical presentations of the 7-dimensional parameter space arising in tessellations of R^3

by Richard Cowan (rcowan@usyd.edu.au) and Viola Weiss (Viola.Weiss@fh-jena.de)

In this paper, we present graphical displays for the theory given in our papers [1] and [2], where we studied tessellations of R^3 , focussing on the non facet-to-facet case (that is, where a cell's facets do not necessarily coincide with the facets of that cell's neighbours). Our paper [1] establishes that the topological parameter space is 7-dimensional and gives numerous formulae that contribute to the combinatorial topology of such tessellations. Paper [2] establishes the inequalities that apply to the 7 parameters and presents many examples. The current supplementary paper shows graphically the form of the constraint space for each example in [2].

The primitive elements of the tessellation are its *vertices*, *edges*, *plates* and *cells* (a “plate” being the closed convex polygon which separates two cells). We assume that the cells are convex polyhedra. To avoid confusion arising because of the clash of notations between *tessellation theory* and *polyhedron theory*, we do not use labels such as “vertex” or “edge” when discussing polyhedral cells. We call a cell's 0-face an *apex*, its 1-face a *ridge* and its 2-face a *facet*. A plate's 0-face and 1-face are called *corner* and *side* respectively, as are the 0- and 1-face of a facet. To resolve any ambiguity here, we say (for example) *plate-side* or *facet-side*.

Three parameters suffice when a tessellation is facet-to-facet. These are (see [1] or [2] for greater formality):

- μ_{VE} := the mean number of edges emanating from the typical vertex;
- μ_{EP} := the mean number of plates emanating from the typical edge;
- μ_{PV} := the mean number of vertices on the boundary of the typical plate.

Our paper [2] gives the constraints on these three parameters, firstly in the facet-to-facet case. These results are new, but it is the non facet-to-facet case which has been our focus --- and that requires four more parameters:

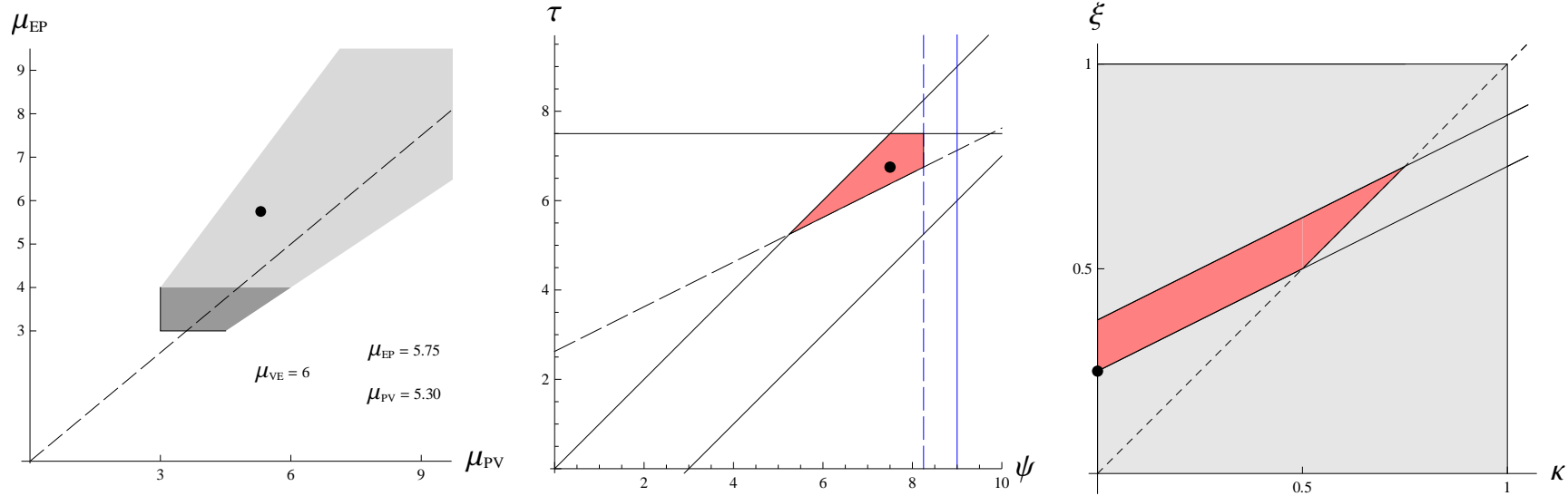
- ξ := the proportion of tessellation edges whose interior is contained in the interior of some facet;
- κ := the proportion of vertices in the tessellation contained in the interior of some facet;
- ψ := the mean number of ridge interiors whose interior contains v , when v is a typical vertex;
- τ := the mean number of plate-sides whose interior contains v , when v is a typical vertex.

See [2] for the algebraic constraints on the 7 parameters and for the detailed definition of each example. See the figures below for a pictorial experience of the constraints. Some examples are facet-to-facet, but many are not.

[1] Weiss, V. and Cowan, R. [Topological relationships in spatial tessellations](#). *Adv. Appl. Prob.* **43**, 963-984 (2011)

[2] Cowan, R. and Weiss, V. [Constraints on the fundamental topological parameters of spatial tessellations](#). Submitted for publication. Also available on ArXiv.

Example 10e. The figures immediately below are given (as Fig. 3) in [2]. They illustrate our strategy to display the 7-dimensional space.



One parameter, μ_{VE} , can take any value ≥ 4 . In Example 10e, $\mu_{VE} = 6$. The grey regions in the left figure show the allowed domain for (μ_{PV}, μ_{EP}) when $\mu_{VE} = 6$. The dark grey region (viewed as “open” on its right boundary, but “closed” on its other boundaries) is the allowed domain for (μ_{PV}, μ_{EP}) in the facet-to-facet case. Non facet-to-facet tessellations can have (μ_{PV}, μ_{EP}) in either the light or dark grey regions (but not on the left or right boundary of the light region nor on the right boundary of the dark region). Note that the light-grey region is unbounded above; it is described by

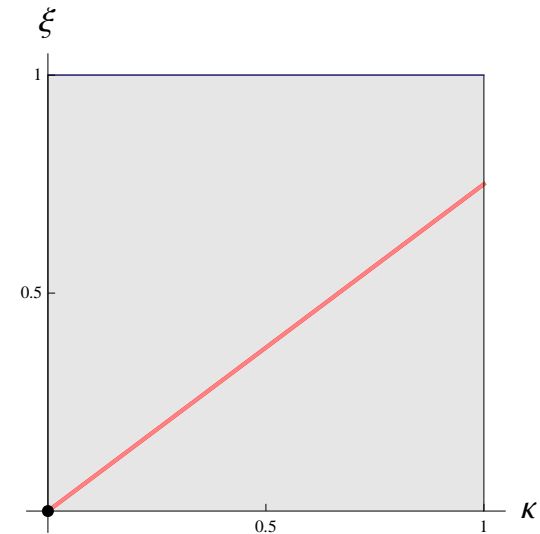
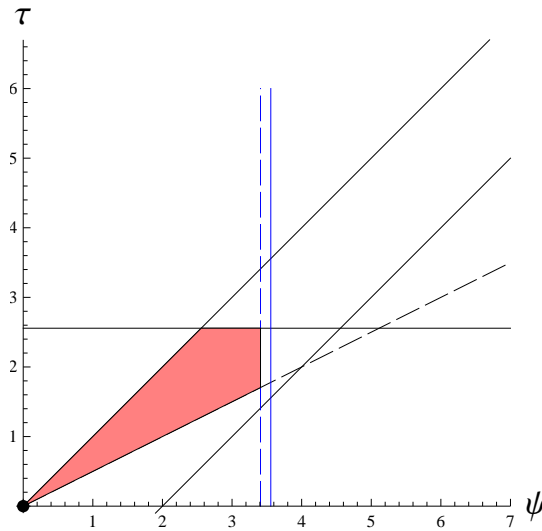
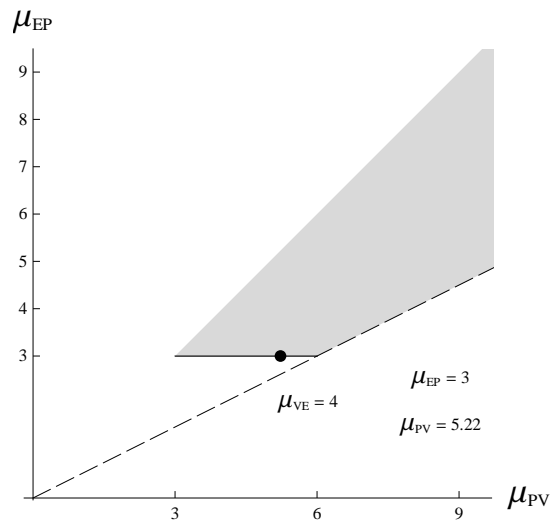
$$\mu_{EP} > 6\left(1 - \frac{2}{\mu_{VE}}\right), \quad \text{combined with} \quad \frac{\mu_{VE} \mu_{EP}}{2(\mu_{VE}-2)} < \mu_{PV} < \frac{\mu_{VE} \mu_{EP}}{\mu_{VE}-2}.$$

The dot in the left figure corresponds to the actual value of (μ_{PV}, μ_{EP}) in Example 10e. Given this value and the value of μ_{VE} , the pink region in the middle figure is the permitted domain for (ψ, τ) . There are 6 constraints (shown as lines) that might be active, in addition to the obvious constraints $\psi \geq 0$ and $\tau \geq 0$. The dot in the middle figure is the actual value in Example 10e of (ψ, τ) . Given the values of $\mu_{VE}, \mu_{EP}, \mu_{PV}, \psi$ and τ , the right figure shows (in pink) the permitted domain for (κ, ξ) . The dot shows the actual value for Example 10e.

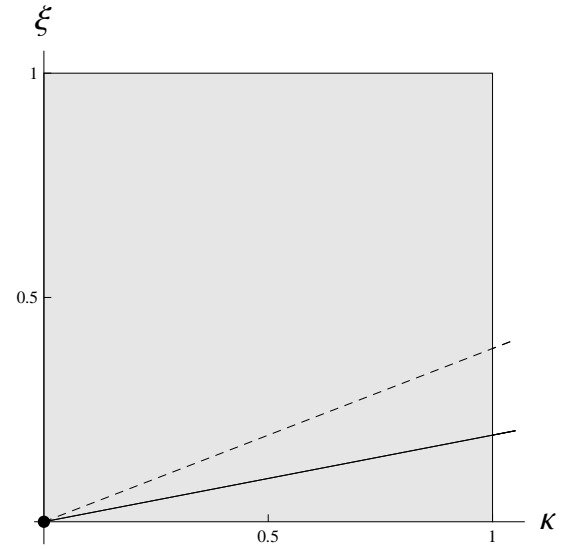
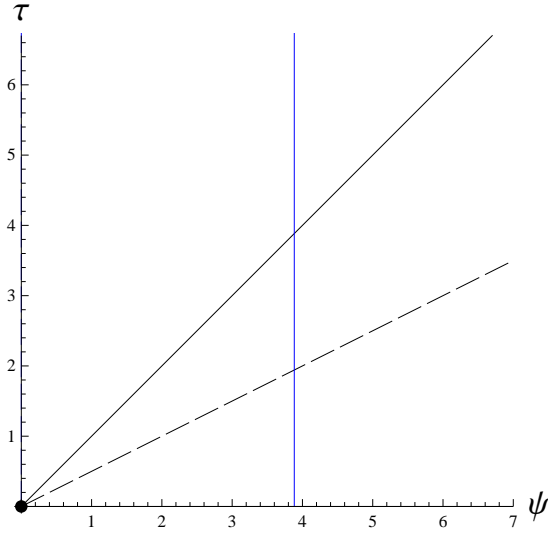
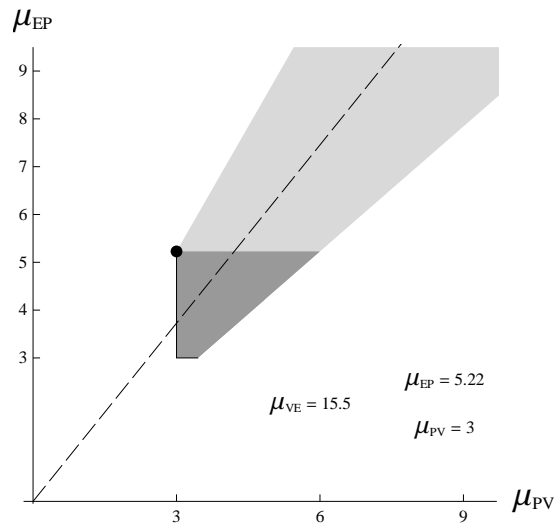
For the meaning of the dashed line in the left picture and the algebraic detail of all the constraining lines, see our paper [2].

The examples in our paper [2]

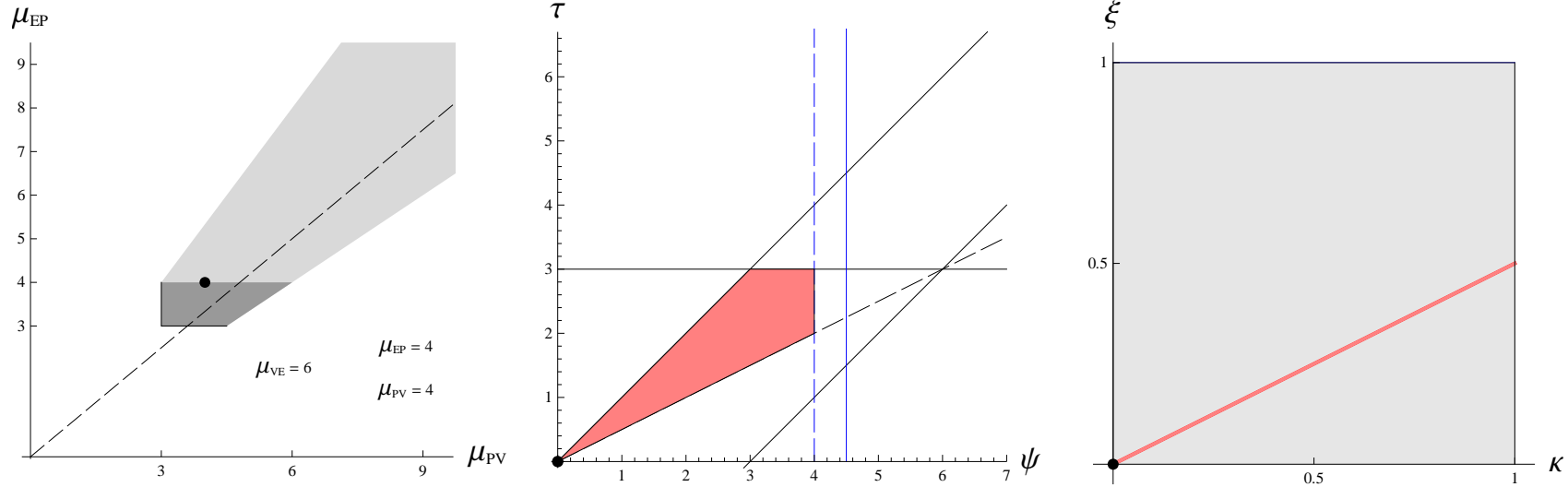
Example 1: Voronoi Note, in the figure above, that the (κ, ξ) domain is bounded above and below by two parallel lines. This is a universal feature in our theory. Sometimes, however, these two lines coincide and the permitted domain becomes a line-segment. Example 1, below, is a case in point. Note also (and this is something independent of the comment above) that the dark grey zone in the left figure below has also been reduced to a line-segment.



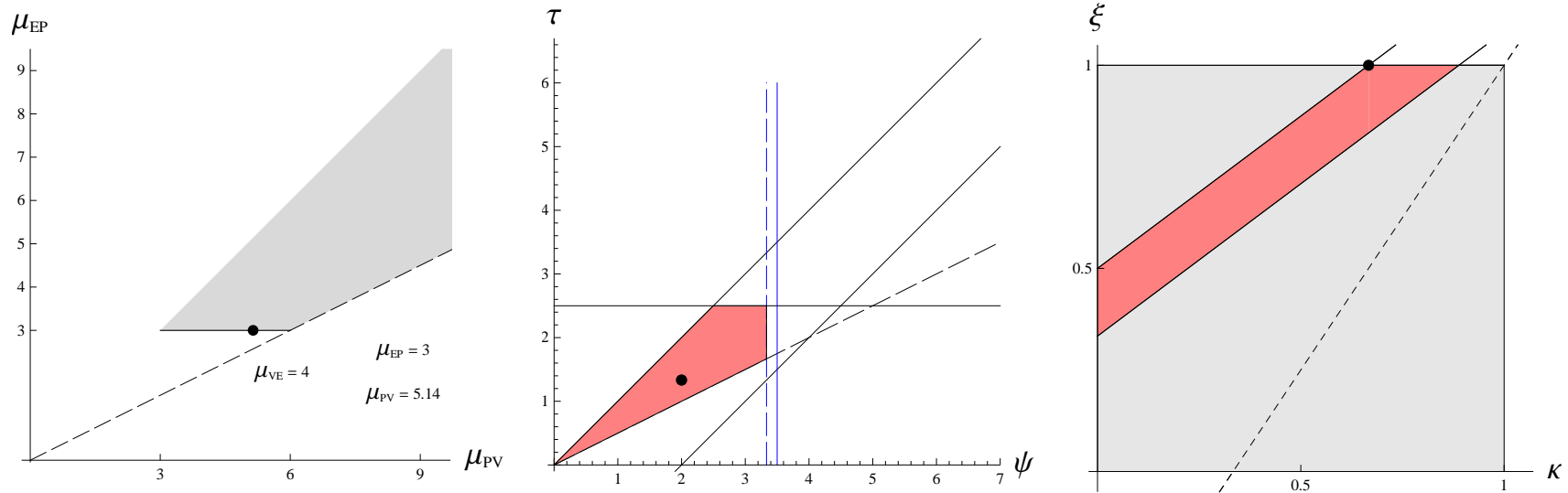
Example 2: Delaunay This example, where every cell is a tetrahedron, produces permitted domains in the middle and right figures which contain only one point, namely $(0,0)$, and we note that the values in Example 2 lie at that point. It is a general fact that if a tessellation is facet-to-facet, and Examples 1 and 2 are, then $\xi = \kappa = \psi = \tau = 0$.



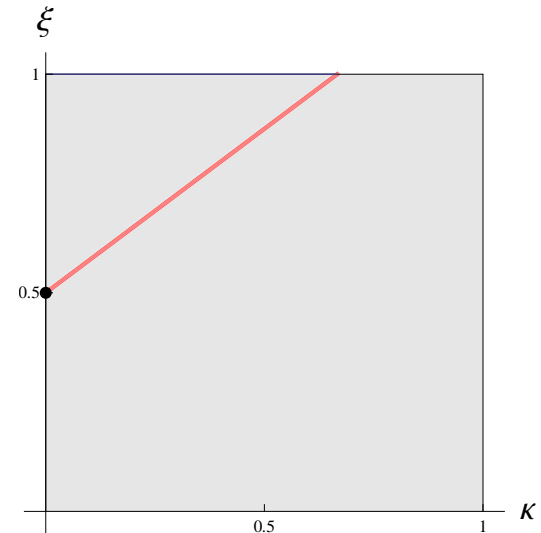
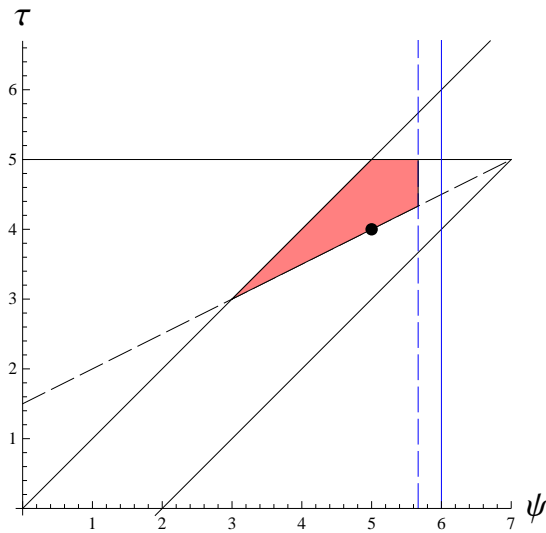
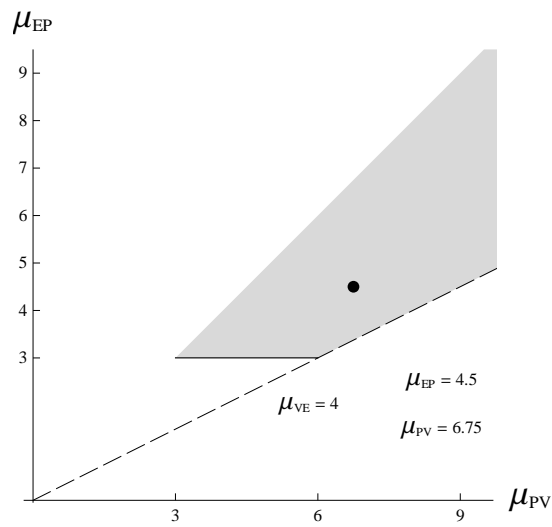
Example 3: Poisson plane process another facet-to-facet tessellation



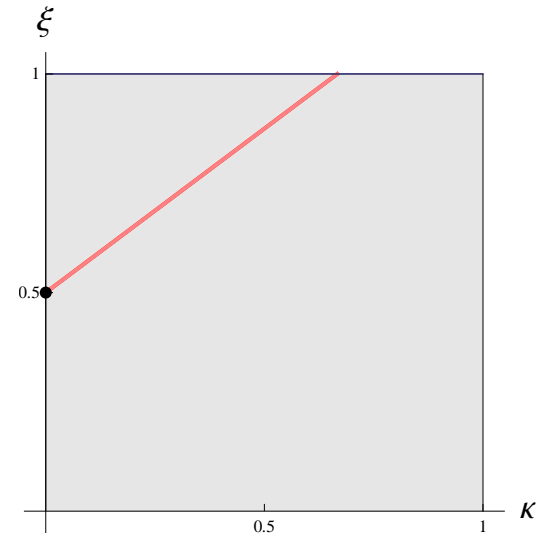
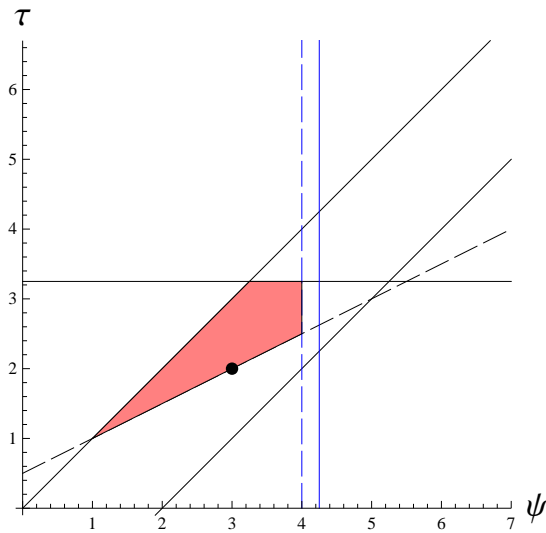
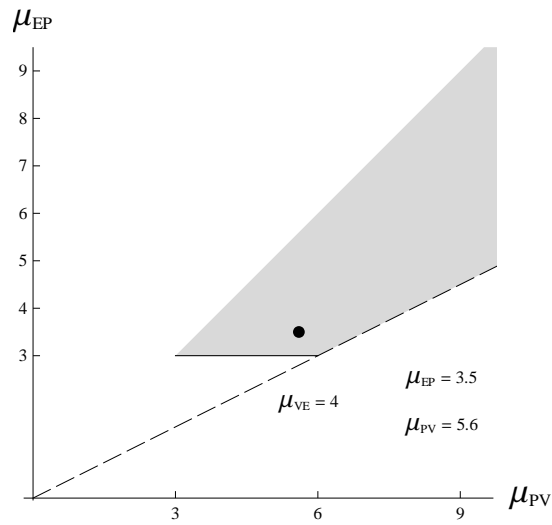
Example 4: STIT one of the most important and best studied non facet-to-facet models



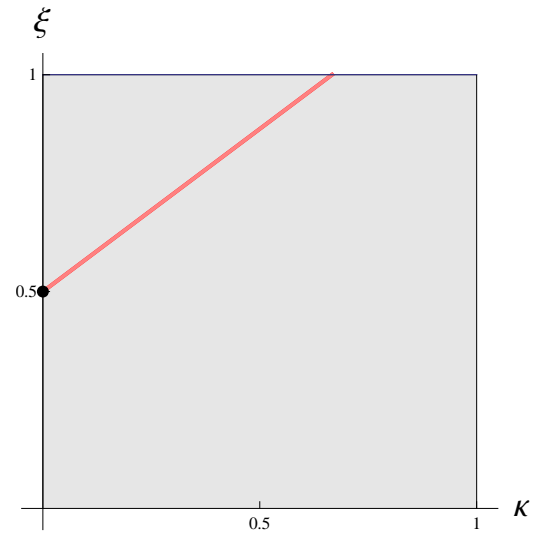
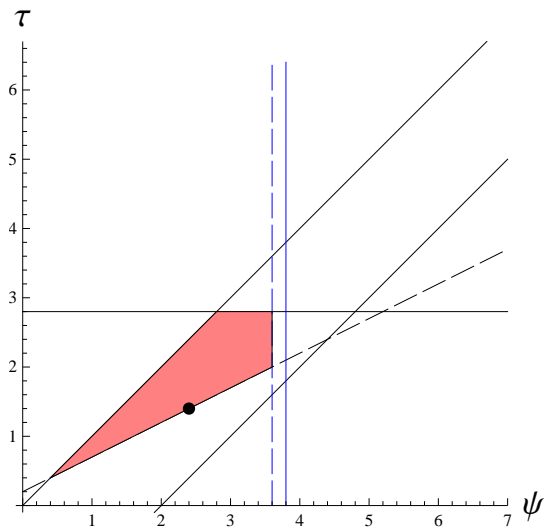
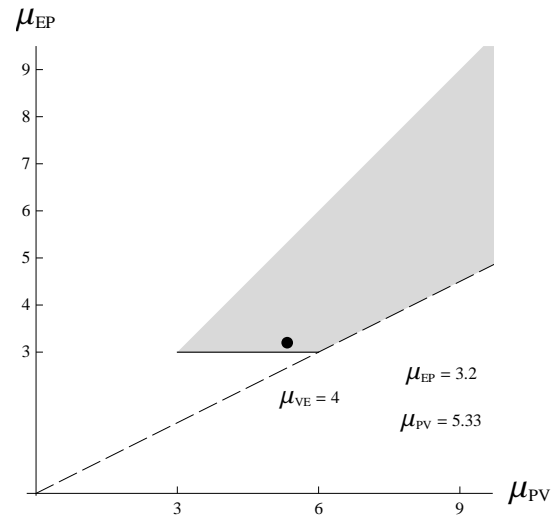
Example 6a: triangular prisms the many cases within Example 6 deal with the so-called “column” models (which comprise columns made from prisms).



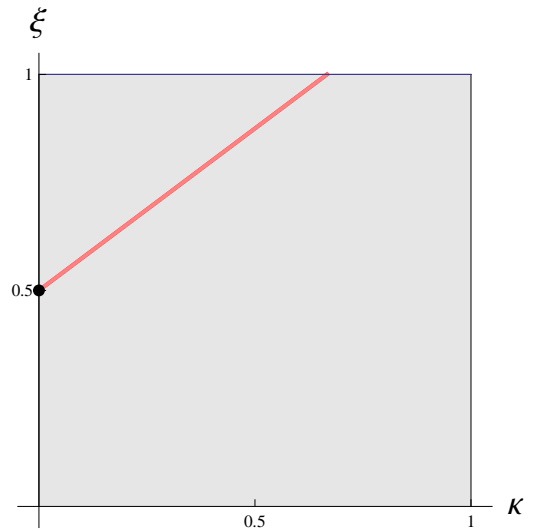
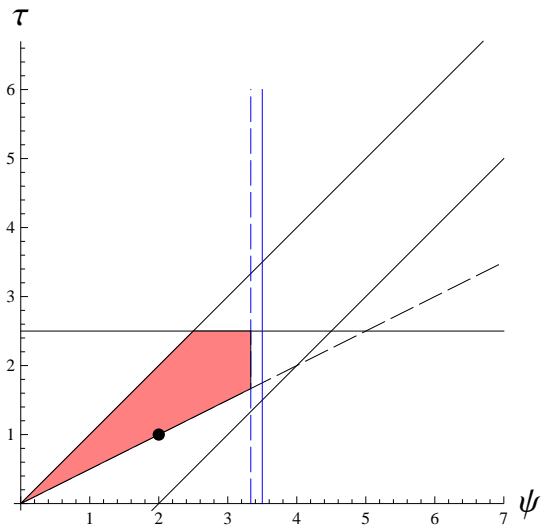
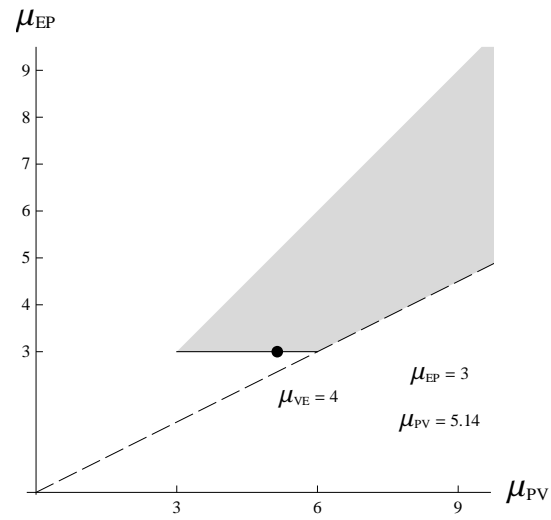
Example 6b: quadrilateral prisms



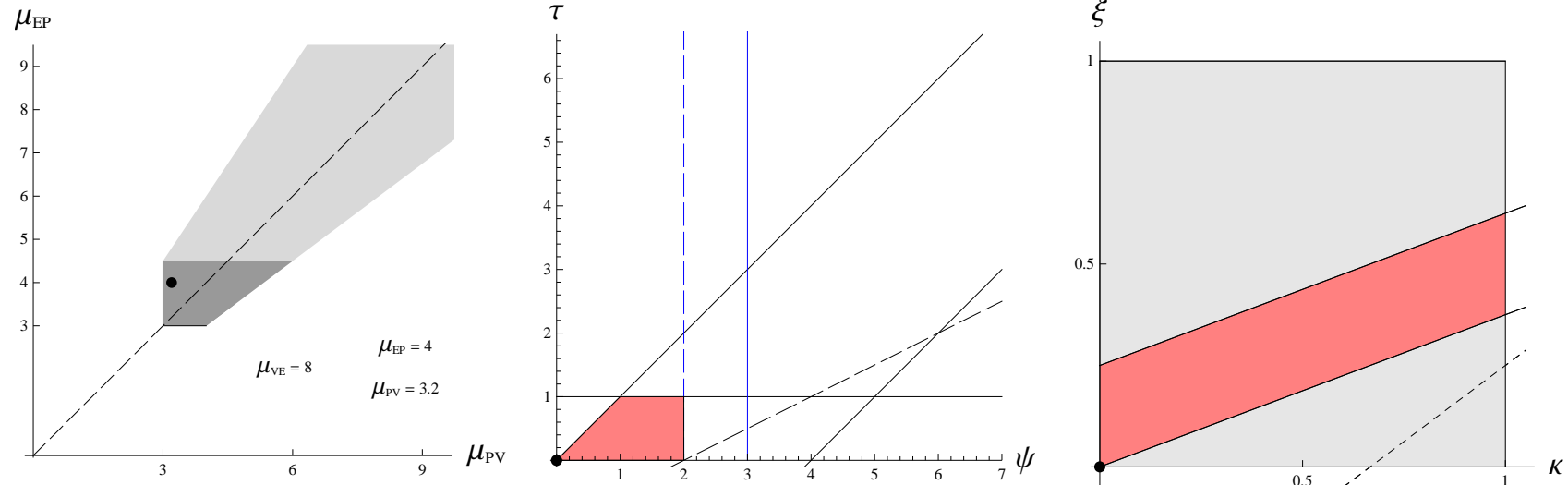
Example 6c: pentagonal prisms (Cairo style, see [2])



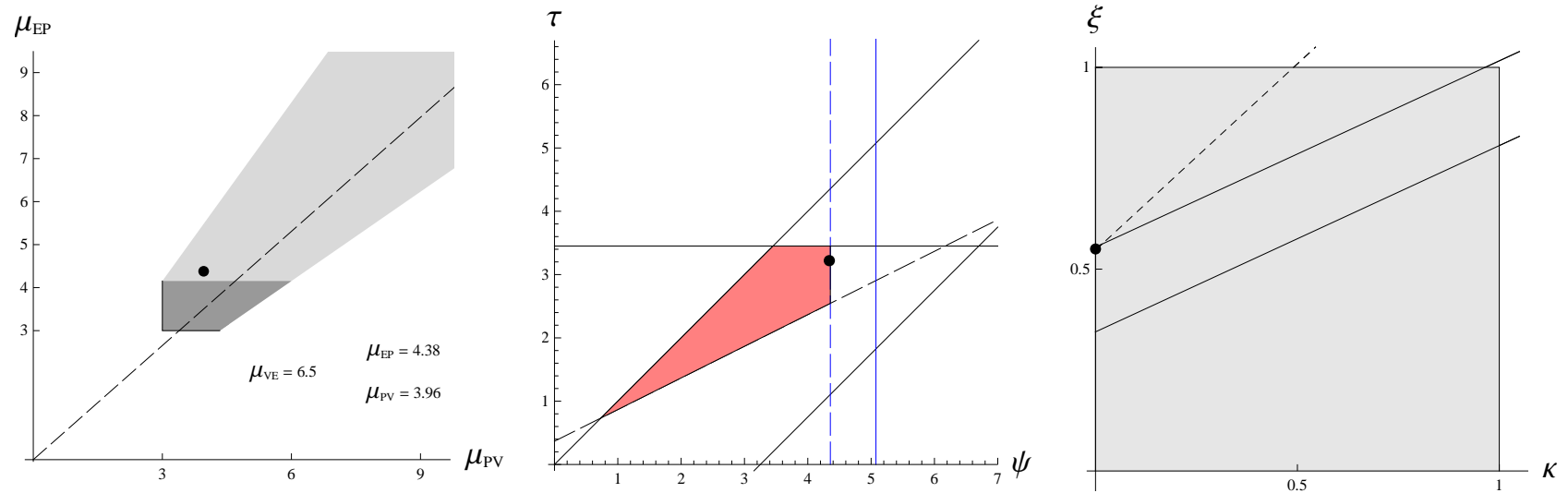
Example 6d: hexagonal prisms



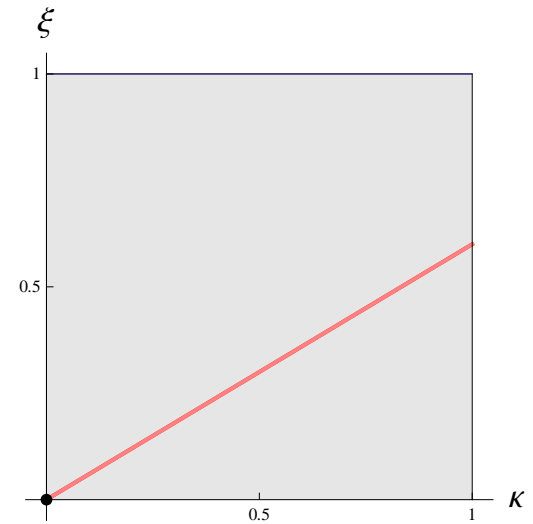
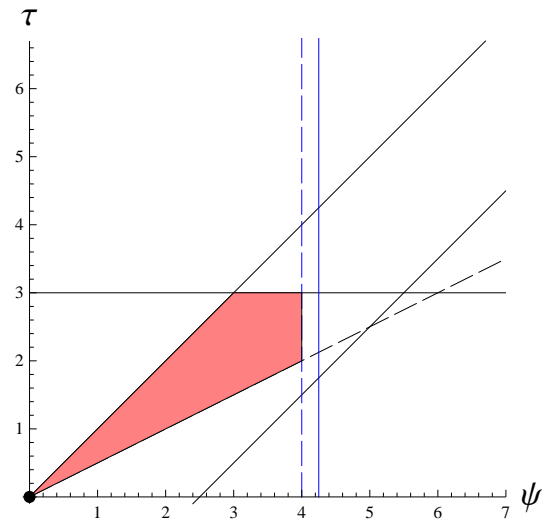
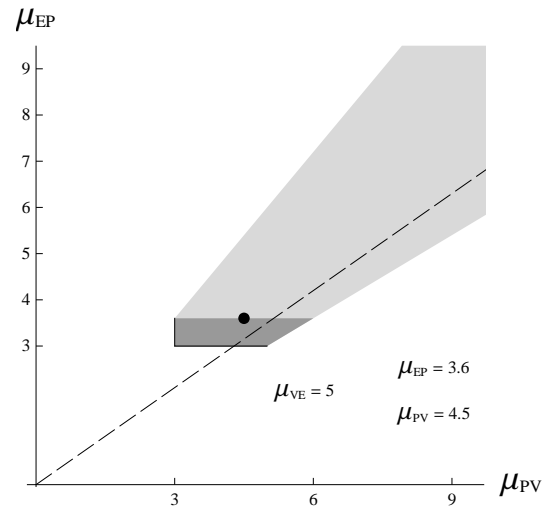
Example 7: Three pyramids cubes partitioned into three congruent pyramids, then packed so that the tessellation is facet-to-facet



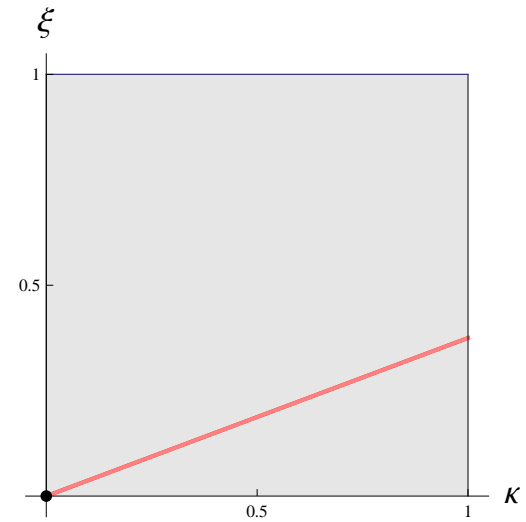
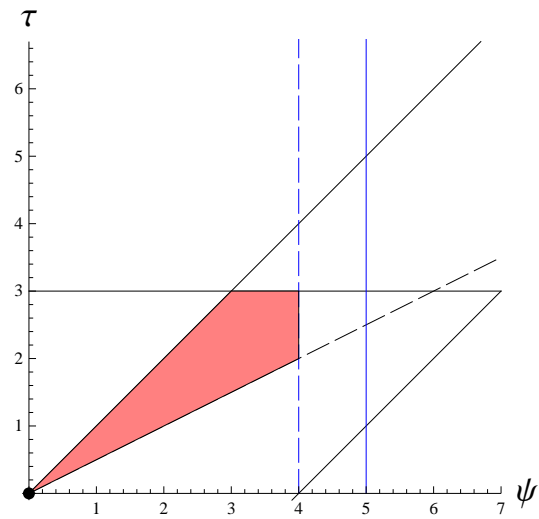
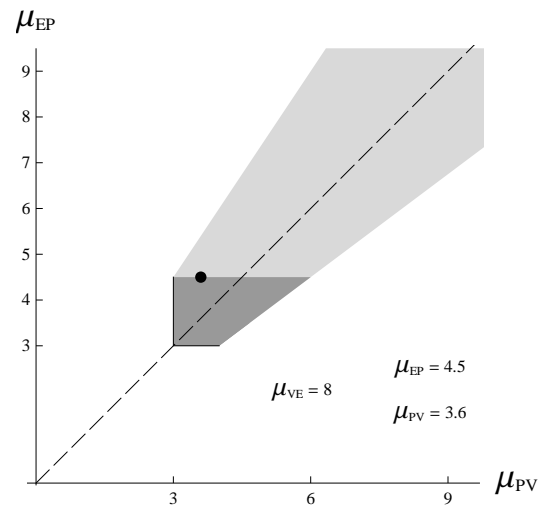
Example 8: Divided Delaunay Here, the right figure looks strange, because the permitted domain for (κ, ξ) has been reduced to one point. This point is the only point which lies on or below the higher of the two parallel constraints AND on or above the dashed constraint.



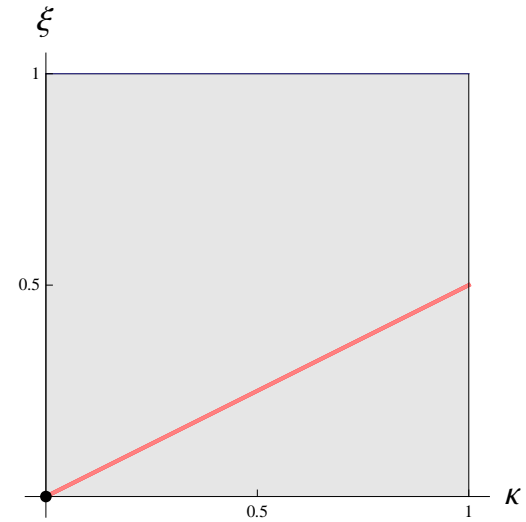
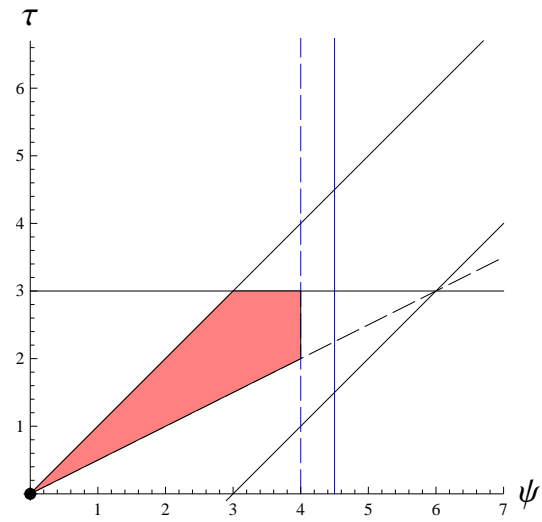
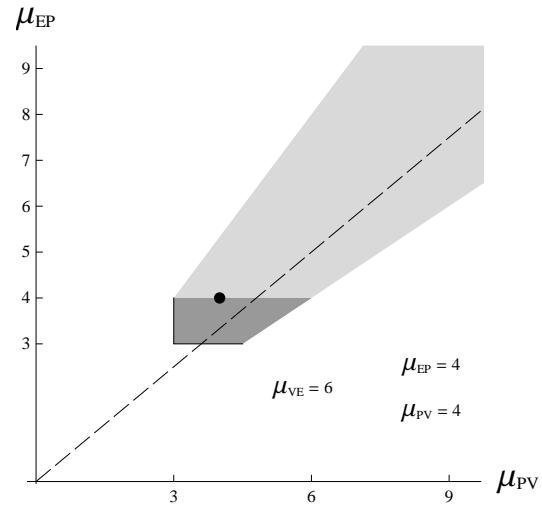
Example 9a: The many cases for Example 9 are based on the so-called “stratum” models, 9a-9c being facet-to-facet.



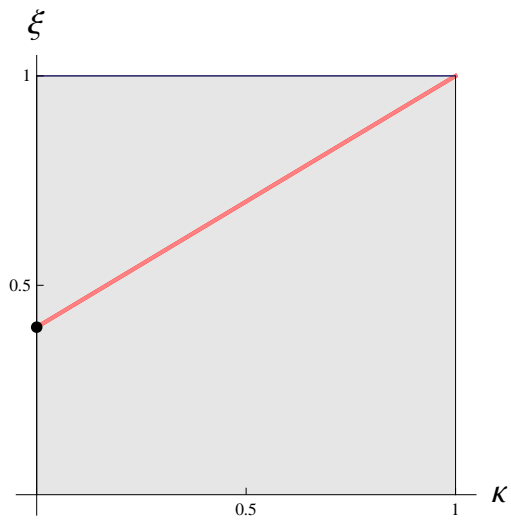
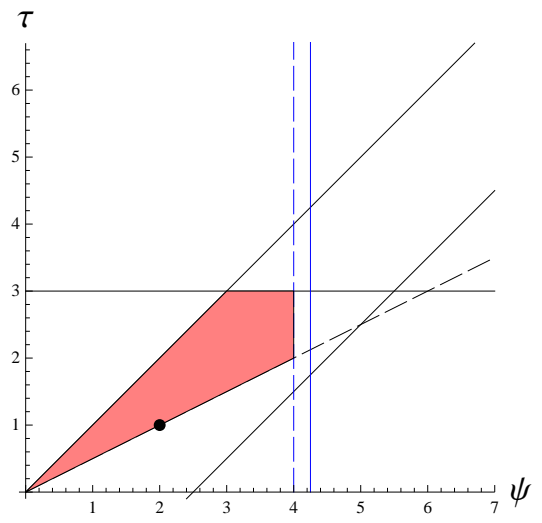
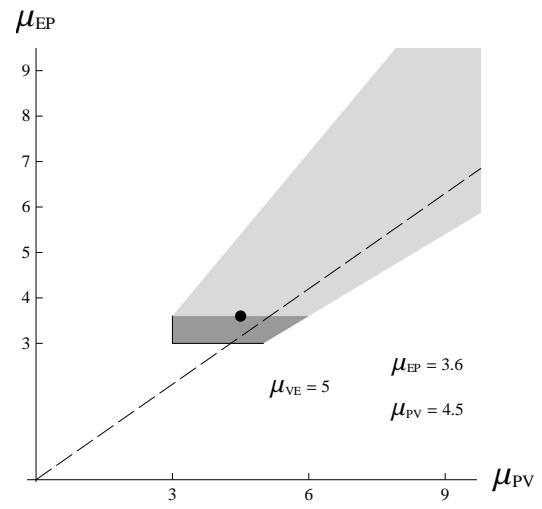
Example 9b:



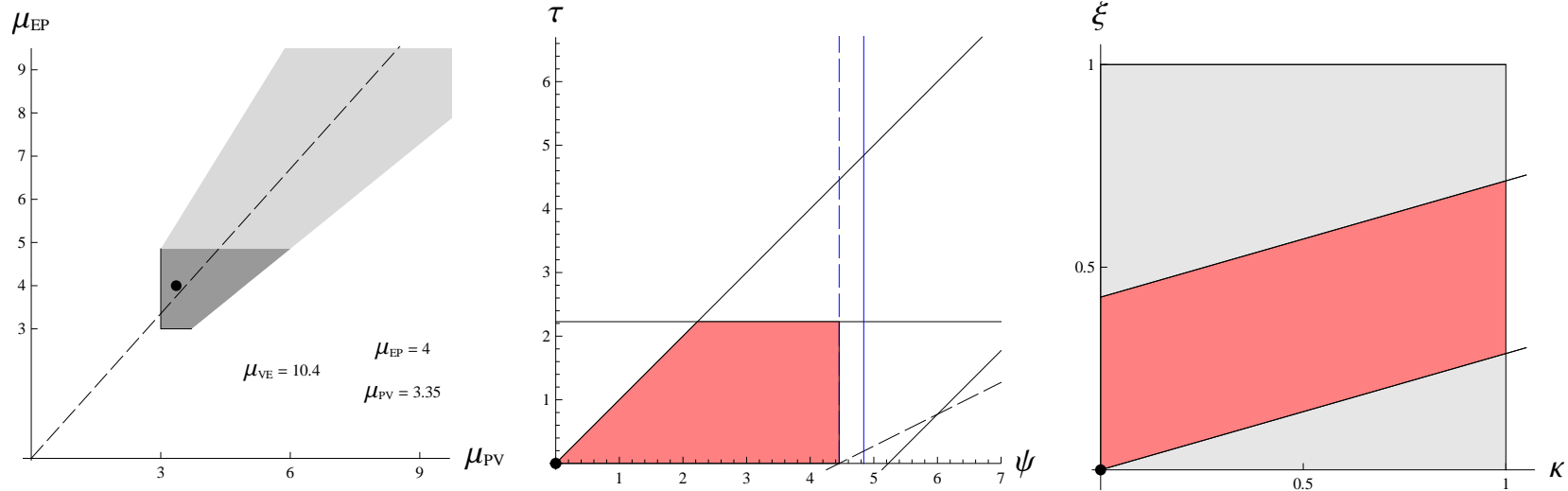
Example 9c:



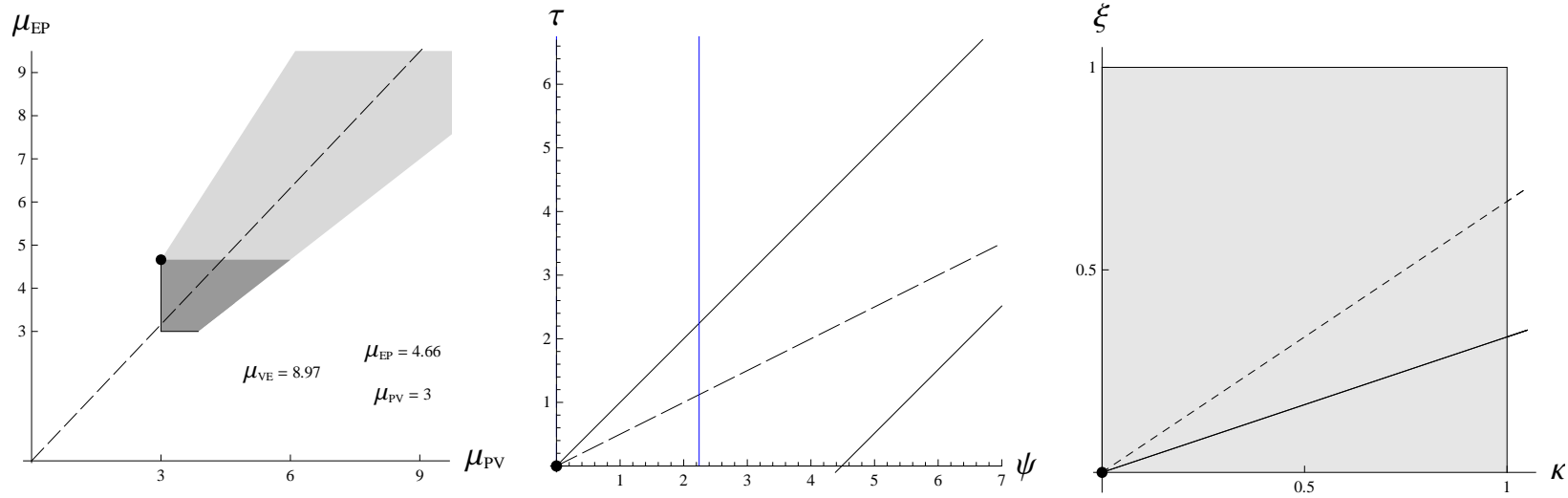
Examples 9d:



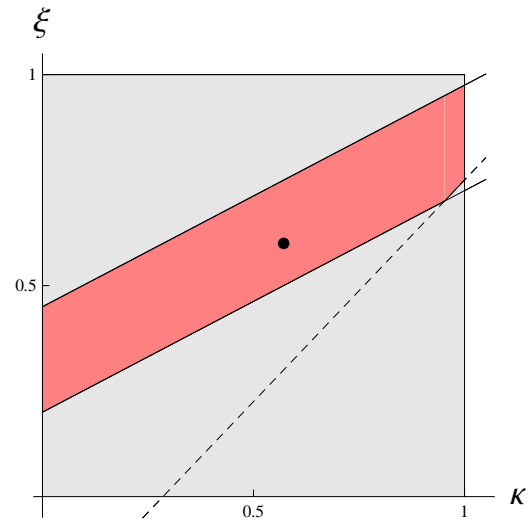
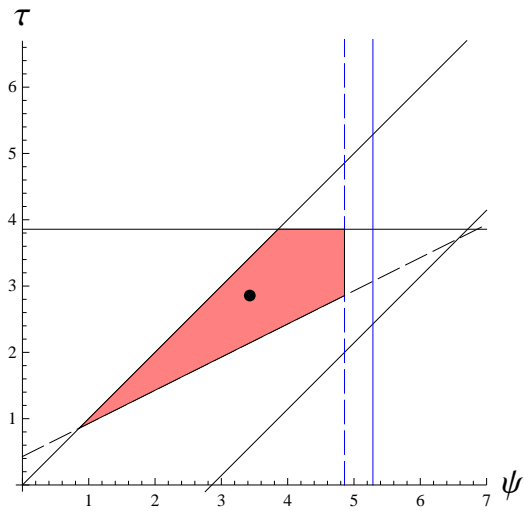
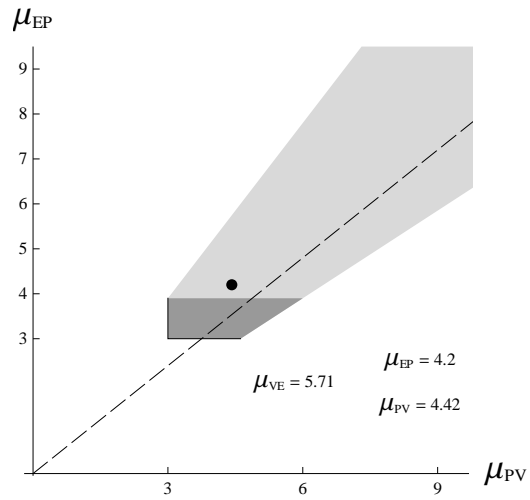
Example 10a:Examples 10 are based on a “central-point” construction



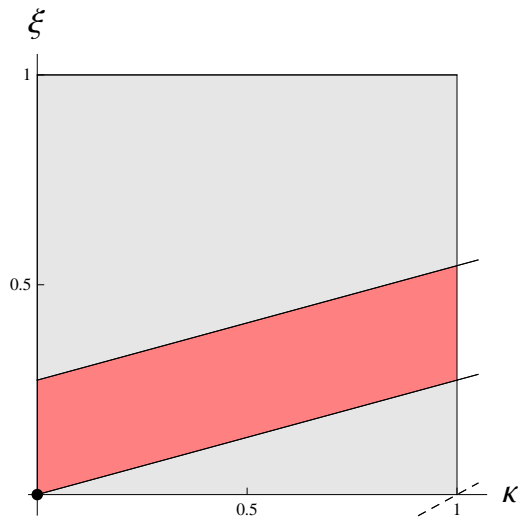
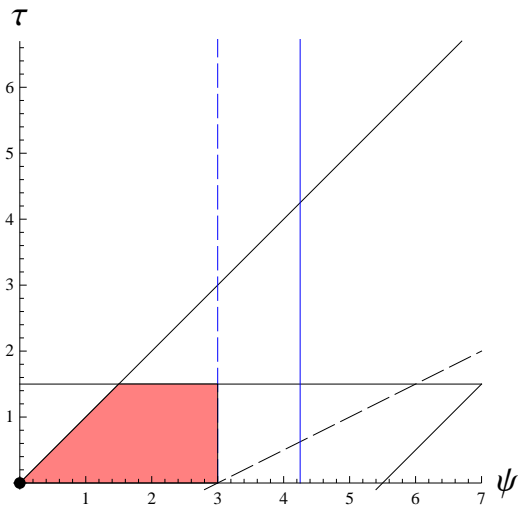
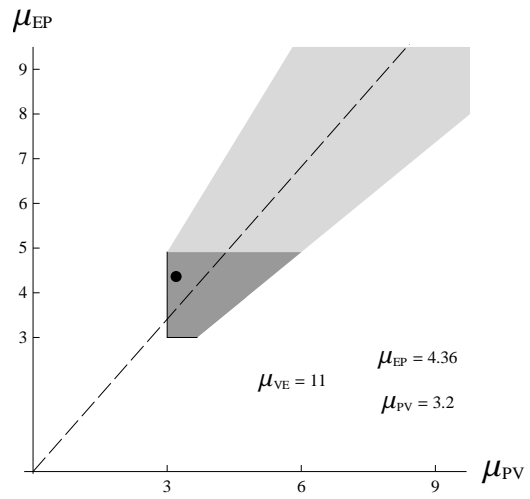
Example 10b: Once again we see the permitted domains collapse to a point in the middle and right figures.



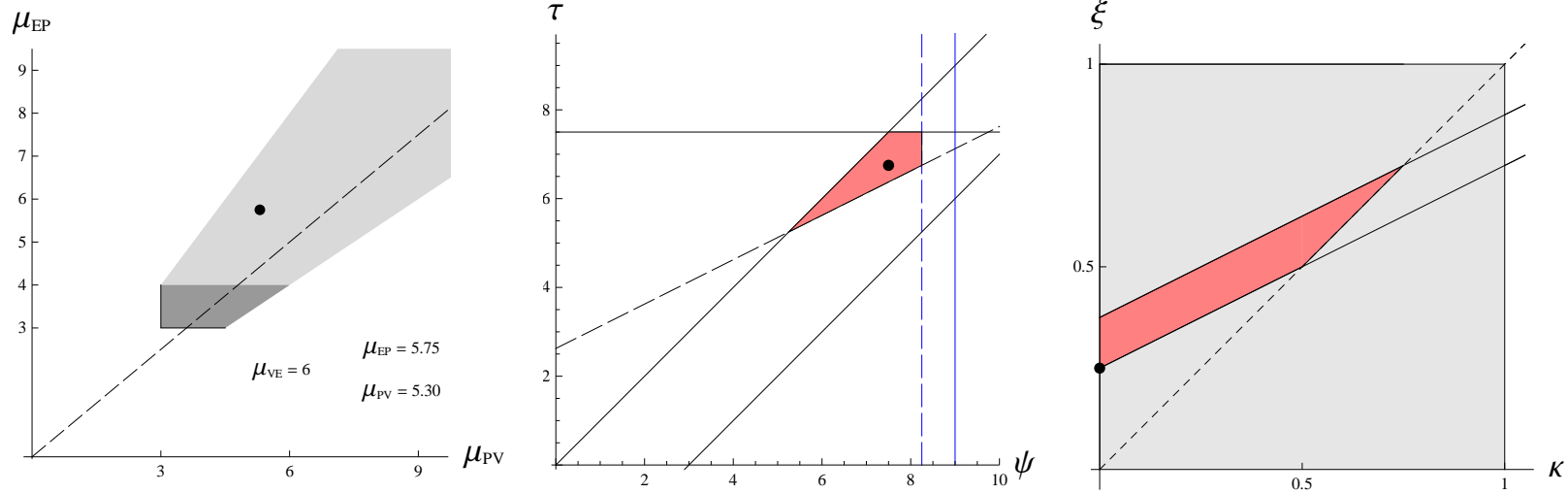
Example 10c:



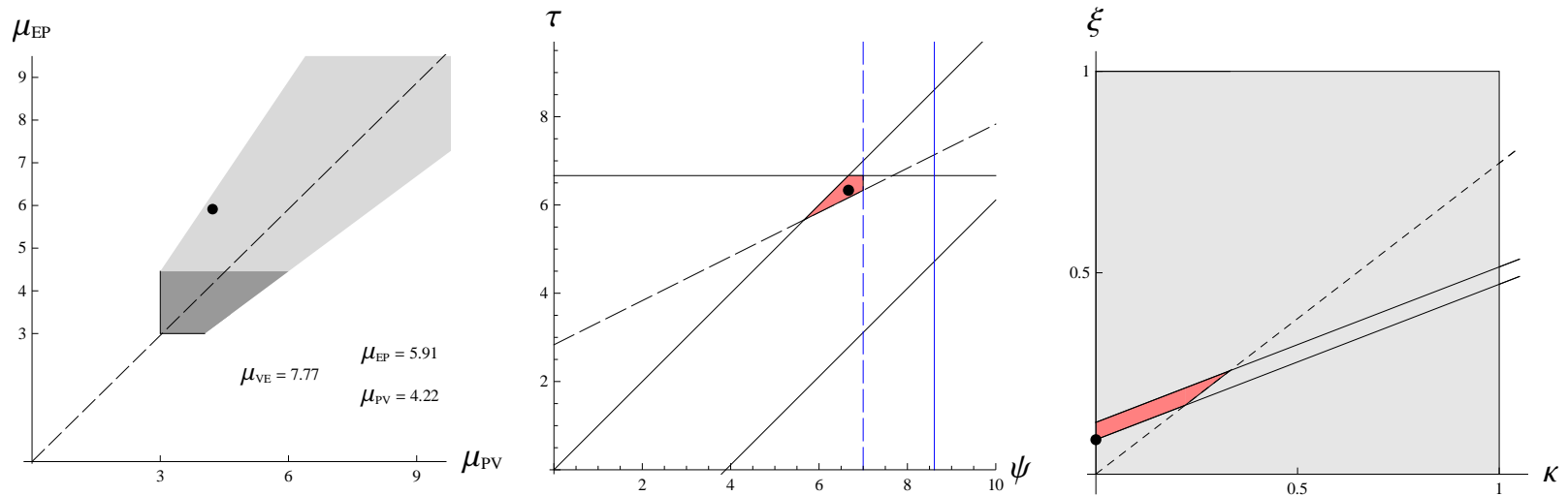
Example 10d:



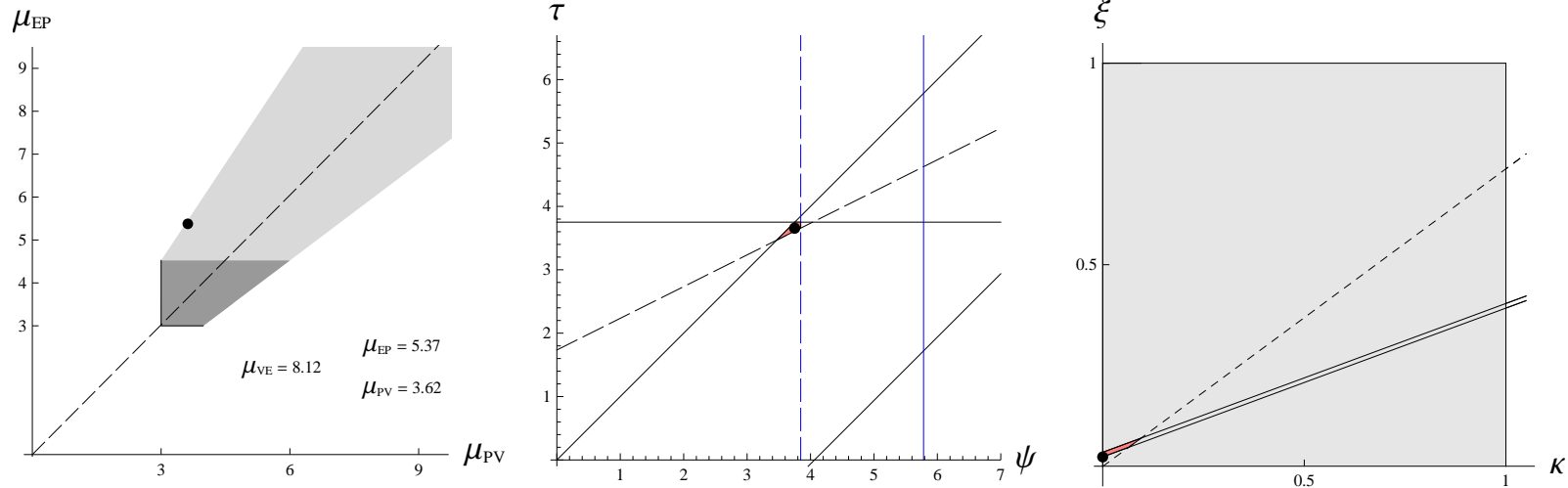
Example 10e: We saw this example at the top of this document.



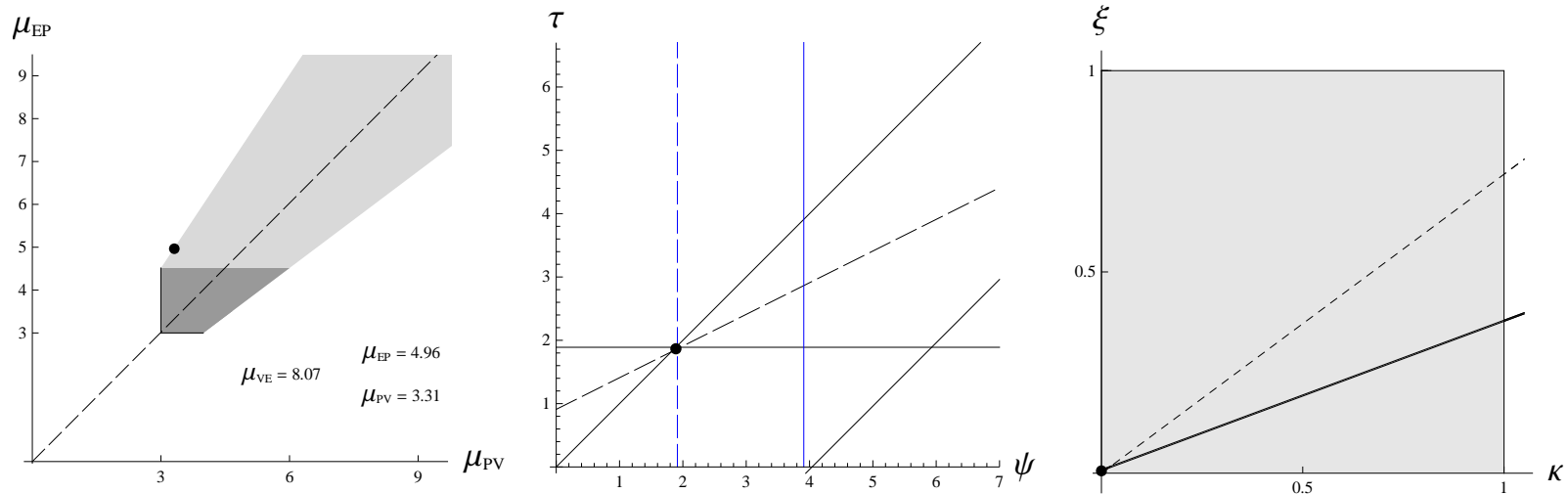
Example 10f: The (μ_{PV}, μ_{EP}) point in the left figure is very close to the “open” boundary of the light-grey region. On this boundary, no tessellations exist and this fact is consistent with the rather small pink domains in the other figures.



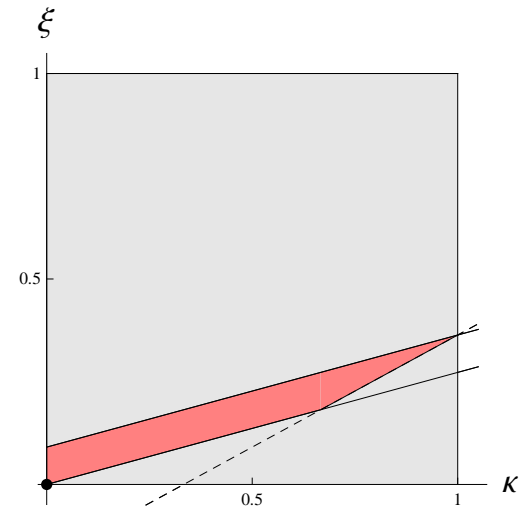
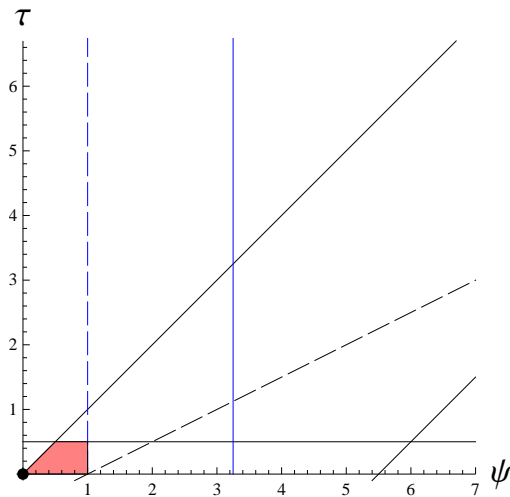
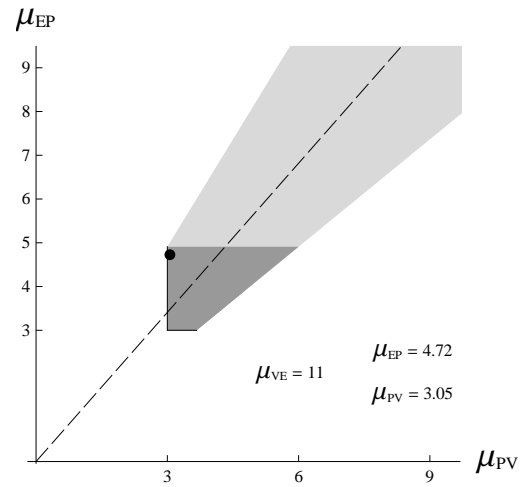
Example 10g: The comment in 10f applies even more so in this example.



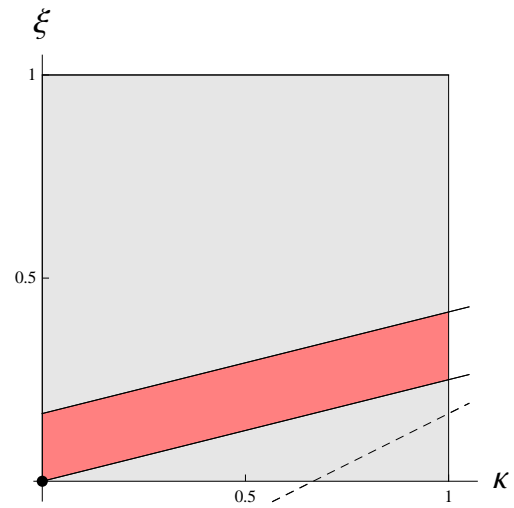
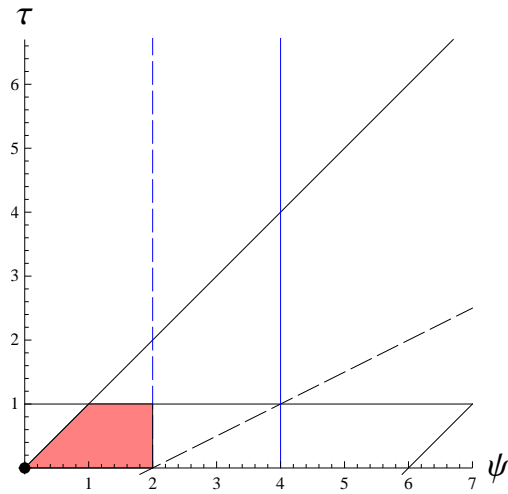
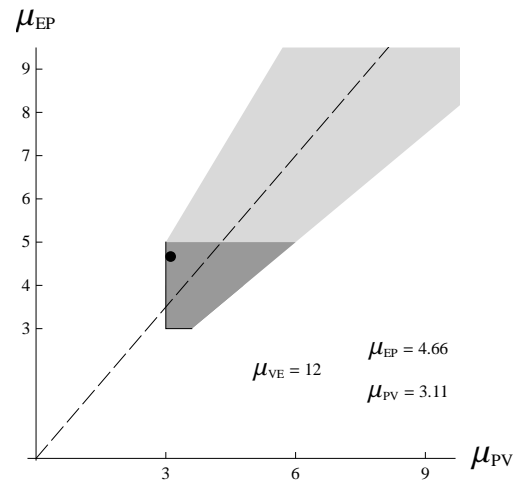
Example 10h: Still more so, here. In this example $\xi = \frac{1}{171}$. The permitted (κ, ξ) domain hasn't quite disappeared.



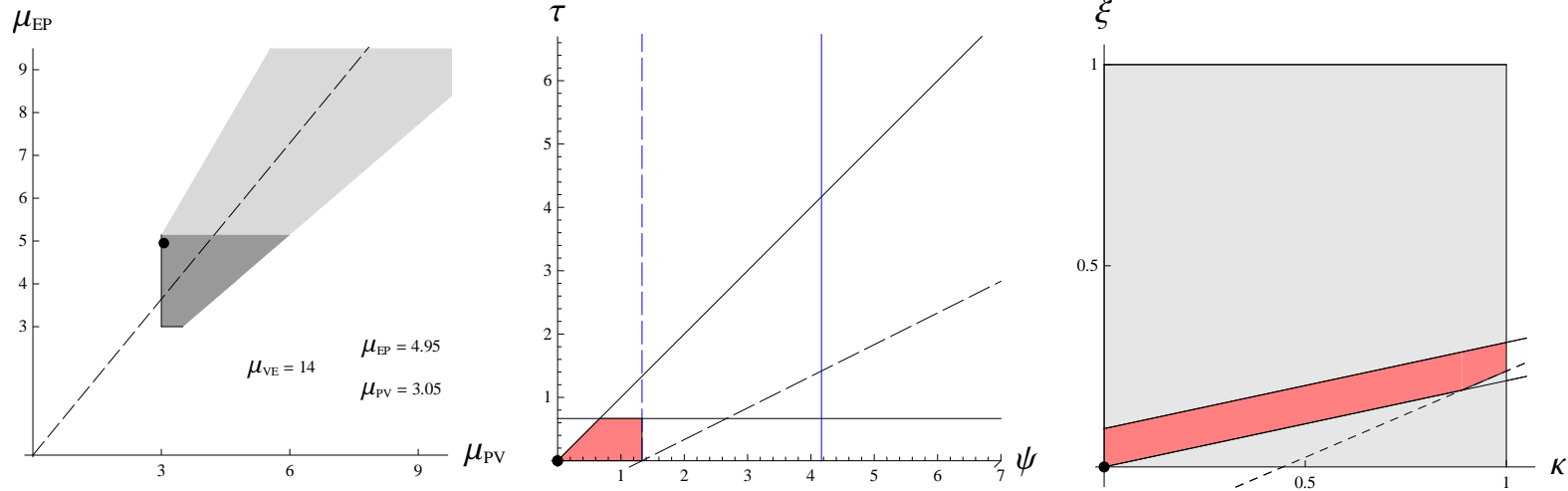
Example 11a:



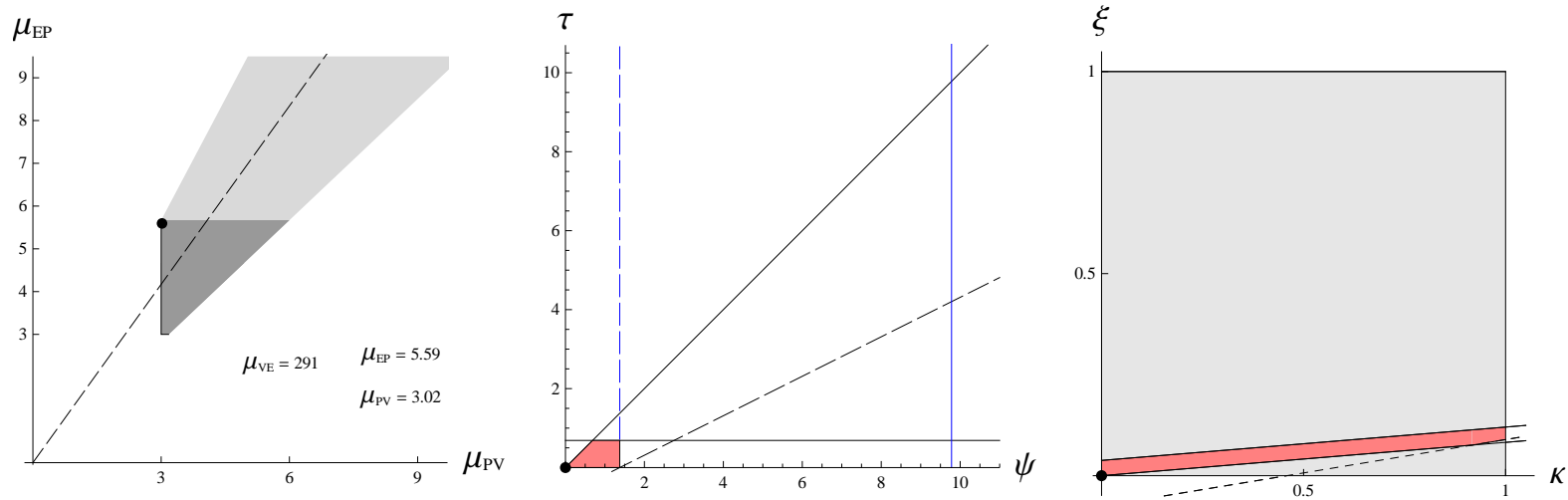
Example 11b:



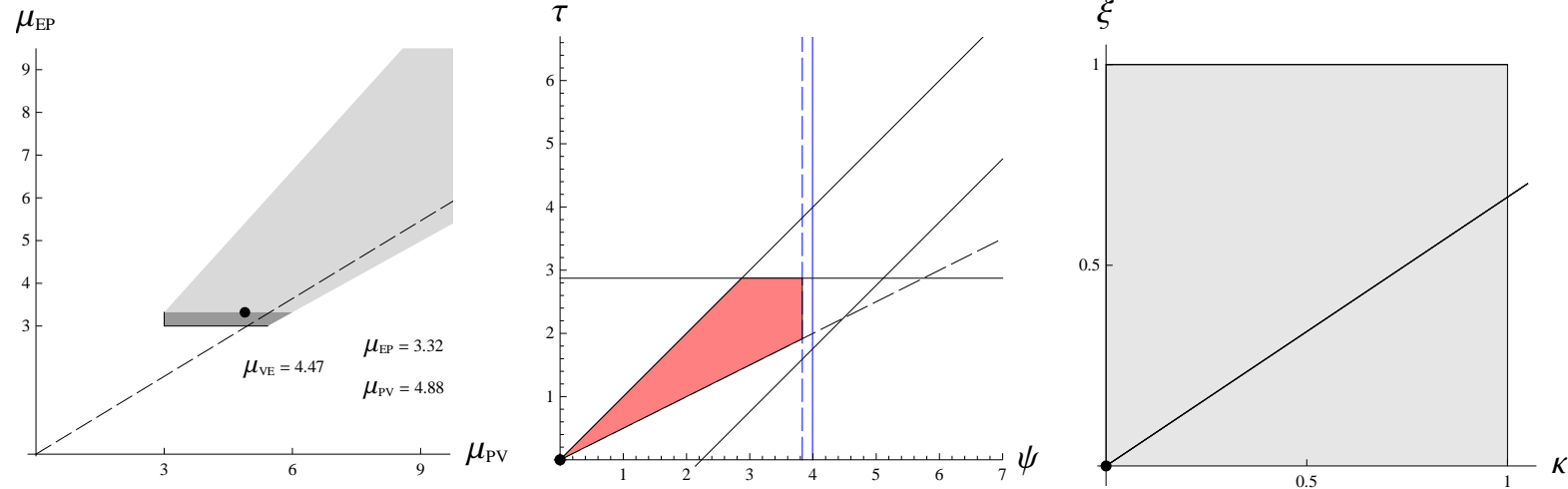
Example 11c:



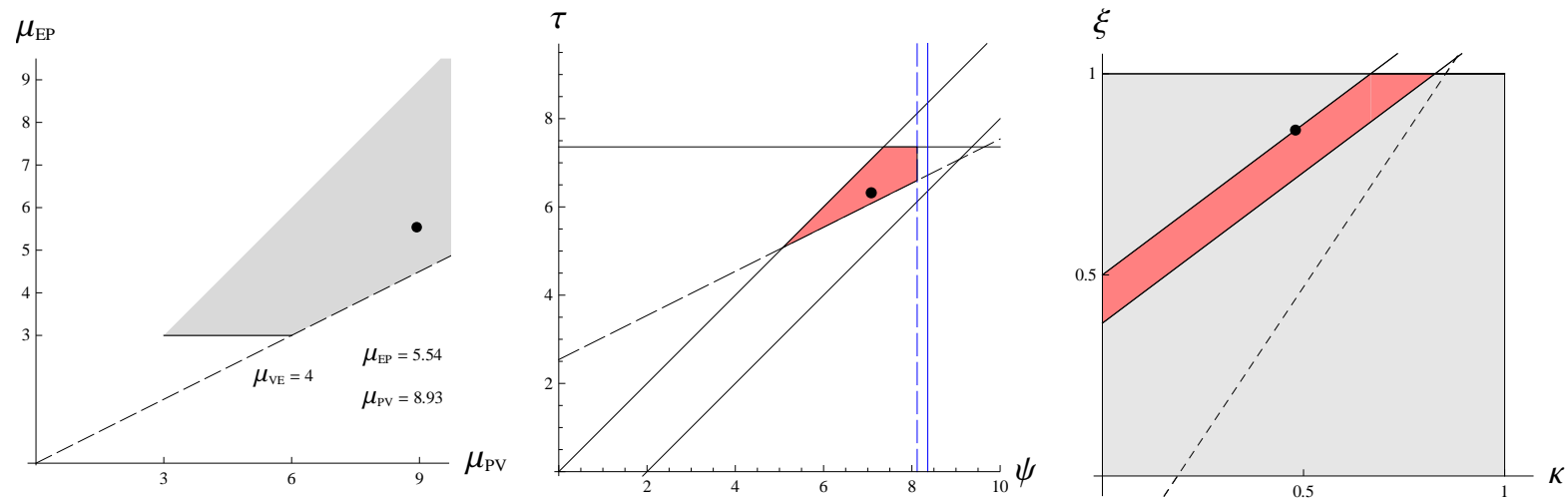
Example 11: another case, with $k=n=10$ (the case $k=n=100$ as mentioned in the construction of Examples 13 is not suitable to plot). Note that μ_{VE} is very large. Our theory (see [2]) proves that μ_{VE} is unbounded above.



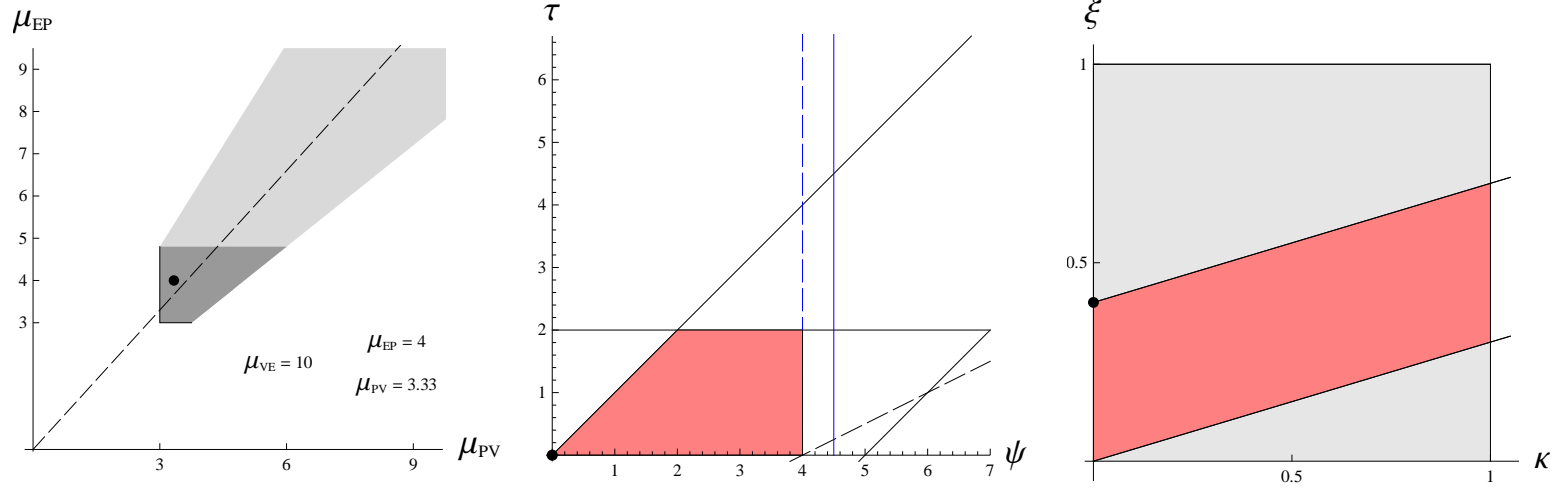
Example 12:



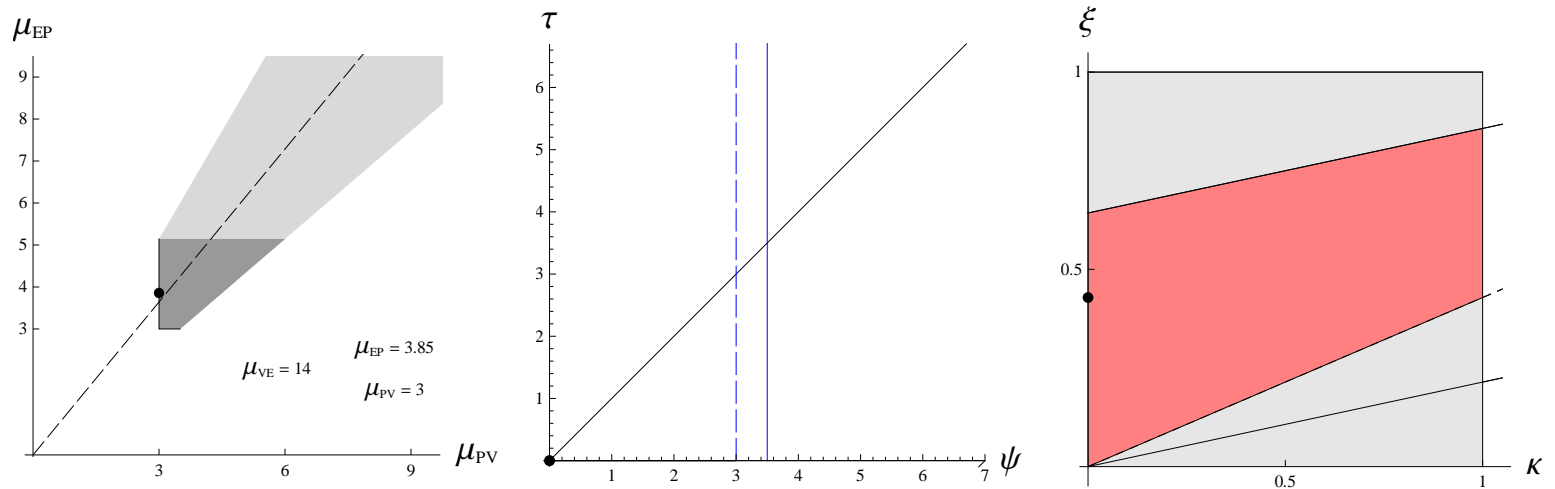
Example 14: (with $n=6$, not $n=8$ as the former has μ_{PV} too high to appear on the left hand plot, without programme changes)



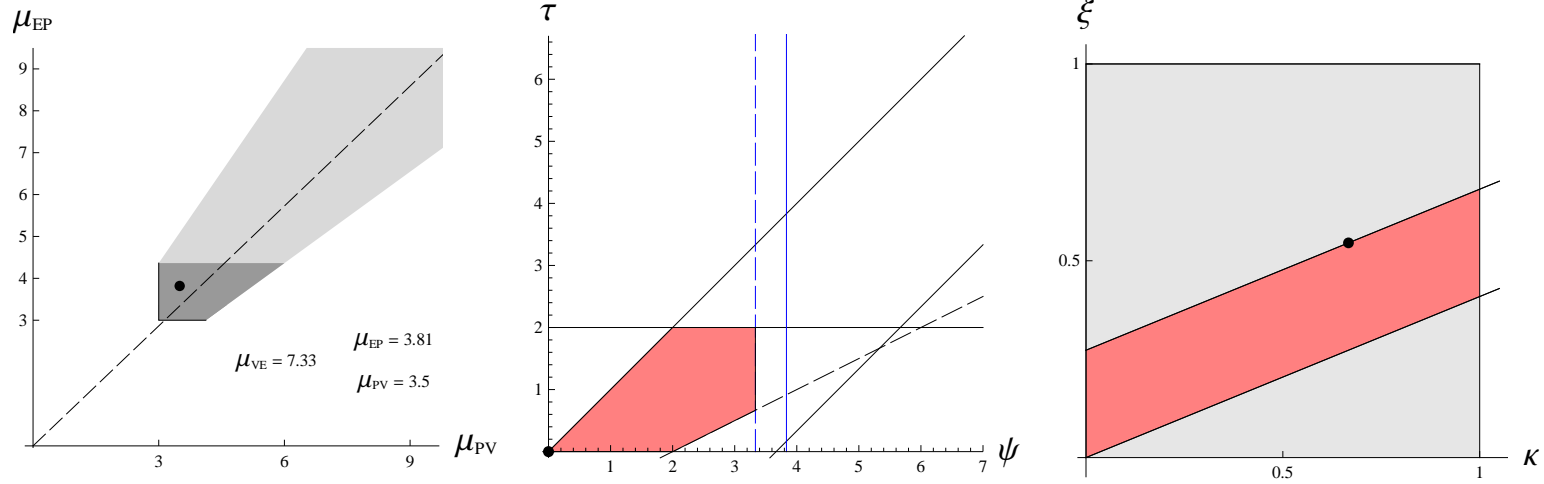
Example 15:



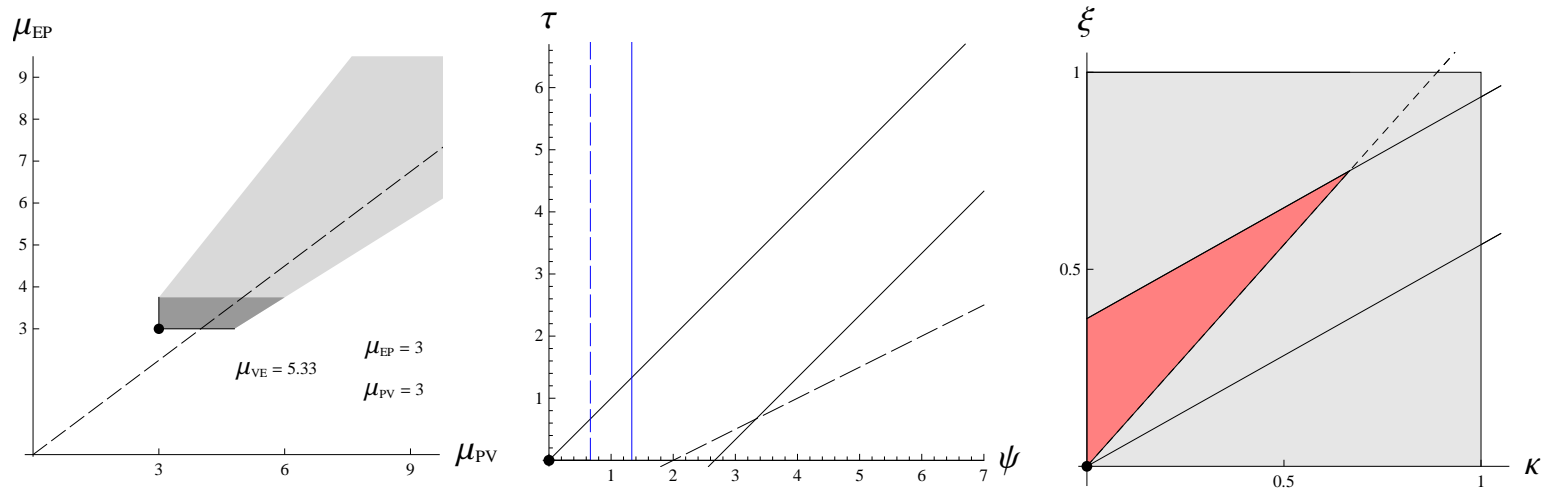
Example 16: Note that the middle permitted zone has collapsed to (0,0).



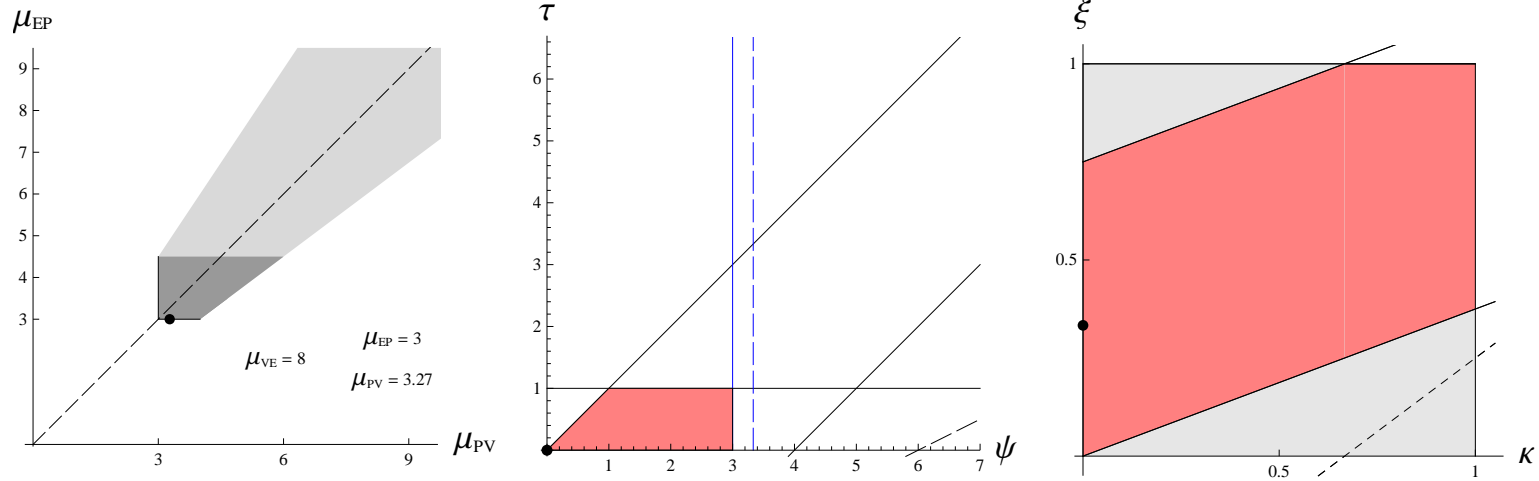
Example 17:



Example 18a: based on a facet-to-facet tiling with congruent copies of the rhombic dodecahedron.



Example 18b: a non facet-to-facet tiling with the rhombic dodecahedron fragmented.



Example 18c: further fragmentation of the rhombic dodecahedron.

